Case Study

Compacted Soil Liner Interface Strength Importance

Timothy D. Stark, F.ASCE[1]; Hangseok Choi[2]; Chulho Lee[3]; and Brian Queen[4]

Abstract: This paper describes an interesting slope failure in a liner system of a municipal solid waste containment facility during construction because the sliding interface is not the geomembrane (GM)/compacted low-permeability soil liner (LPSL) but a soil–soil interface within the LPSL. Some of the lessons learned are as follows: (1) compaction of the LPSL should ensure that each lift is kneaded into the lower lift so a weak interface is not created in the LPSL; (2) the LPSL moisture content should be controlled so it does not exceed the specified value, for example 3–4% wet of optimum, because it can lead to a weak interface in the LPSL; (3) drainage material should be placed over the GM from the slope toe to the top to reduce the shear stresses applied to the weakest interface; and (4) equipment should not move laterally across the slope if it is unsupported but up the slope while placing the cover soil from bottom to top. **DOI: 10.1061/(ASCE)GT.1943-5606.0000556.** *© 2012 American Society of Civil Engineers.*

CE Database subject headings: Slope stability; Landfills; Geomembranes; Geosynthetics; Shear strength; Liners.

Author keywords: Slope stability; Landfills; Geomembranes; Geosynthetics; Compacted soil liner; Geosynthetic lined slopes; Interface shear strength.

Introduction

Hazardous and municipal solid waste (MSW) landfills in the United States are required to have a low hydraulic conductivity composite liner system with an overlying drainage system. The liner system usually consists of compacted low permeability soil and geosynthetic materials. The stability of these liner systems is controlled by the shear strength of the each component and the various component interfaces present in the system. There have been many examples of slope instability by weak geosynthetic interfaces, such as the Kettlemean Hills hazardous waste facility (Stark and Poeppel 1994; Stark et al. 1998). In addition, many researchers (e.g., Martin et al. 1984; Saxena and Wong 1984; Koerner et al. 1986; Williams and Houlihan 1987; Negussey et al. 1989; Bove 1990; Mitchell et al. 1990; O'Rourke et al. 1990; Takasumi et al. 1991; Yegian and Lahlaf 1992; Stark and Poeppel 1994; Stark et al. 1996; Dove and Frost 1999; Stark and Choi 2004; Dixon et al. 2006; Amaya et al. 2006) have shown that geomembrane (GM) and geosynthetic interface shear resistance can be low and usually lower than soil–soil interface shear resistance. This widespread knowledge of the low shear resistance of GM and geosynthetic interface strengths makes this case history noteworthy.

This case history is interesting because the sliding interface is not the GM/compacted low permeability soil liner (LPSL) interface, but it is a soil–soil interface within the LPSL. It is interesting that a soil–soil interface would be weaker than the overlying GM/LPSL interface even with a double-sided textured GM and during placement of the overlying drainage material because of the low normal stress acting on the GM/LPSL interface. However, the photographs presented in this paper show that the sliding occurred on the soil–soil interface within the LPSL and not on the GM/LPSL interface. This case history is important for designers and third-party construction quality assurance (CQA) and construction quality control (CQC) personnel to encourage them to carefully inspect soil–soil interfaces to ensure limited lift thickness is used so that the compaction equipment, for example, sheepsfeet, and energy can penetrate the entire lift and the part of the underlying lift so a weak interface is not left in the LPSL.

This paper reviews the initial design, construction, and slide movement that resulted in this slope failure. Afterward, the paper provides analyses and recommendations to help avoid this problem in future projects.

Site Description and Construction

The site is located in the preglacial Teays River Valley in Ohio. This preglacial river was dammed up during the advance of the Pleistocene glaciers causing the river to be partially filled with fine sand, silt, and clay. The fluvial deposits at the site range from 0- to 25-m thick and are mostly clay with liquid limits ranging from 45 to 56, more than 95% passing the 200 sieve, and 55–73% smaller than 0.002 mm. This clay soil was used to construct the LPSL discussed subsequently.

During construction activities on November 14, 2001, a slope failure occurred in a nominal three Horizontal to one Vertical 3H:1V sideslope of the MSW landfill. The composite liner system consists from bottom to top of

[1]Professor, Dept. of Civil and Environmental Engineering, Univ. of Illinois, 205 North Mathews Ave., Urbana, IL 61801. E-mail: tstark@illinois.edu

[2]Associate Professor, School of Civil, Environmental, and Architectural Engineering, Korea Univ., Anam-Dong, Seongbuk-Gu, Seoul 136-713, South Korea (corresponding author). E-mail: hchoi2@korea.ac.kr

[3]Postdoctoral Research Associate, School of Civil, Environmental, and Architectural Engineering, Korea Univ., Anam-Dong, Seongbuk-Gu, Seoul 136-713, South Korea. E-mail: cryfreer@korea.ac.kr

[4]Environmental Engineer, Ohio Environmental Protection Agency, Southeast District Office, 2195 Front St., Logan, OH 431381. E-mail: brian.queen@epa.state.oh.us

Note. This manuscript was submitted on August 4, 2009; approved on April 18, 2011; published online on April 20, 2011. Discussion period open until September 1, 2012; separate discussions must be submitted for individual papers. This paper is part of the ***Journal of Geotechnical and Geoenvironmental Engineering***, Vol. 138, No. 4, April 1, 2012. ©ASCE, ISSN 1090-0241/2012/4-544–550/$25.00.

Downloaded 01 May 2012 to 130.126.241.238. Redistribution subject to ASCE license or copyright. Visit http://www.ascelibrary.org

- A 1.5 m (5 ft) of LPSL,
- A 1.5-mm (60 mil) thick, double-sided textured high-density polyethylene (HDPE) GM, and
- A 0.3–0.6 m (1–2 ft) of protective/drainage sand material.

Figs. 1 and 2 are photographs of sideslope construction and show the liner system installed and granular drainage layer (GDL) placed from the top to the bottom of the slope. This placement practice is not recommended because the GDL is unbuttressed and imparts high shear stresses on the liner system and the weakest liner system interface because of the weight of the GDL and equipment operating on the inclined slope (Giroud et al. 1995; Koerner and Soong 1998; Stark and Choi 2004). As a result, it is frequently recommended that GDL be placed from the bottom to the top of the slope so that the GDL buttresses itself and reduces the shear stresses and shear displacement applied to underlying liner system interfaces (Giroud et al. 1995; Koerner and Soong 1998; Stark and Choi 2004). This top to bottom placement technique was especially problematic in this case because the slope is fairly long, so a considerable thickness of material had to be pushed from the top to the bottom of the slope. Figs. 1 and 2 show that the unbuttress thickness of GDL near the slope toe is substantial and ranges in thickness from 1 to 1.5 m (3–5 ft). This large thickness can impart large shear stresses in the liner system and on the weakest interface.

Fig. 1. Overview of failed slope and folded geomembrane at slope toe

Fig. 2. Overview of sideslope and protective sand placement on geomembrane

The GDL was stockpiled by large, off-road dump trucks at the crest (top) of the slope. The GDL stockpiles at the crest were 1.5–2.4-m (5–8 ft) high in some cases. Two low ground pressure (LGP) bulldozers (CAT D6 and John Deere 850) were used to move material from the crest down the slope as shown in Fig. 2. The dozers were assumed to exert a ground pressure of 34.4 kPa (720 psf) on the basis of manufacturers, literature. In the area of the failure, the dozers made a number of lateral passes on the slope instead of maintaining top to bottom or bottom to top passes, while spreading the sand cover material. This resulted in the equipment and drainage material remaining unsupported across the slope as the equipment moved laterally across the slope. Granular drainage layer was not spread on the lower third of the slope at the time of the failure as shown in Fig. 2.

It was observed that the slope failure occurred as a series of block slides with the top block failing first and subsequent blocks failing as the upper block overrode the next lower block. In particular, the first failure began approximately 3 m (10 ft) below the slope crest where one dozer was operating. The toe of this slide was located approximately 12 m (40 ft) down the slope from the crest. A second slide started at the toe of the upper most slide and extended approximately 12 m farther down the slope. A third slide started at the toe of the second slide and extended approximately 12 m farther down the slope. In summary, the slide started near the slope crest and pushed from the top to the bottom as each slide block thrust over the next. Thus, a progressive failure of the entire slope occurred because the upper slide block transferred its stresses to the next block, which failed and transferred its stresses to the next slide block until the entire slope became involved in the slide.

There were no observations of GM distress before the first slope failure. The GM distress would have been apparent because the cover soil was placed from the top down (see Fig. 2), so GM would have started to accumulate at the slope toe, but none was visible.

Fig. 3 is a photograph near the toe of the slope and shows the damaged GM because of the slope movement. This type of GM damage is typical in slope movement situations because the GM easily tears under the large applied shear and normal stresses.

Fig. 4 is a photograph from upslope of the slide movement. This photograph shows the drainage material overlying the torn GM and the sliding surface below the torn GM. The failure surface was primarily confined to a depth of 75–150 mm (3–6 in.) into the compacted LPSL interface but not at the GM/LPSL interface. More importantly, Fig. 4 shows that the failure or slickensided surface extended the entire length of the slide because the drainage material and GM are missing from upslope of where the slide mass stopped (see arrow in Fig. 4) to where the slide block stopped.

The arrow in Fig. 4 also shows the location of the photograph in Fig. 5. Fig. 5 is a close-up photograph of the torn GM that clearly shows the slide surface occurring below the torn GM. From Fig. 5, it may be concluded that sliding occurred in the compacted LPSL first and the GM was torn as a result of this movement. A back-analysis using the software SLOPE/W was conducted and

Downloaded 01 May 2012 to 130.126.241.238. Redistribution subject to ASCE license or copyright. Visit http://www.ascelibrary.org

Fig. 3. Photo of failed slope and damaged geomembrane

Fig. 4. Photo of slide surface and torn geomembrane

Fig. 5. Close-up of torn geomembrane that shows the slide surface is below the geomembrane/LPSL interface

incorporates the tensile resistance of the GM and the interface strength of the GM/LPSL interface.

Fig. 6 is a photograph of the exposed sliding surface in the compacted LPSL. This photograph shows striations in the LPSL that confirms the location of sliding was in the LPSL. In addition, a footprint is evident that indicates the soft and moist nature of the surface of the LPSL.

Fig. 6. Close-up photo of slide surface in the LPSL

Observations of the sliding surface indicate that the sliding surface does not correspond to a specific compacted lift interface. This is evident because the sliding surface is only approximately 75–150 mm (3–6 in.) into the compacted LPSL. Generally, a lift interface is not within 75–150 mm at the top of the compacted LPSL unless some additional material was placed on the top lift so the final LPSL thickness meets the regulatory requirement of approximately 1.5 m (5 ft) or final grade. As shown in Fig. 6, the failure surface was "slickensided," that is a "polished" appearance, which is caused by clay-particle reorientation into face-to-face/parallel arrangements. This occurs when large strains or displacements are experienced along a well-defined failure surface (Amaya et al. 2006; Stark and Choi 2004; Stark et al. 2005).

The compaction specification for the LPSL to achieve a saturated, vertical hydraulic conductivity of less than 1×10^{-7} cm/s is a relative compaction of 95% or greater on the basis of standard Proctor compaction (ASTM D698) and a moisture content of $> 1\%$ wet of optimum. The maximum dry unit weight and optimum moisture content for the LPSL soil are 15.8 kN/m^3 (100.3 pcf) and 21.6%, respectively. Daily Field Compaction Reports provide insight into the compaction procedure that includes a maximum loose lift thickness of approximately 200 mm (8 in.), compacting each lift with a minimum of 12 one-way passes by using a sheepsfoot compactor, and no clods are included. Table 1 presents a summary of the dry unit weight and moisture content for Lifts 3–6. Lift 6 corresponds to the top of the LPSL. The compaction data shown in Table 1 were obtained by using a nuclear density gauge, and all the tests for Lifts 3–6 passed the requirements of $\geq 95\%$ standard proctor relative compaction and a moisture content of $\geq 1\%$ optimum or $\geq 22.6\%$. On the basis of the Daily Field Compaction Reports, test results indicate that the LPSL was compacted for Lifts 5 and 6 at a upper bound moisture content that is slightly greater (26.7%) than for Lifts 3 and 4 (26.5 and 25.5%). In addition, the average moisture contents for Lifts 5 and 6 (25.4 and 26.0%) are also slightly higher than for Lifts 3 and 4 (25.0 and 24.2%). Thus, the moisture content of Lifts 5 and 6 appears slightly higher than Lifts 3 and 4.

After the slide, four moisture content specimens were obtained from the exposed slide surface as shown in Fig. 6. The measured moisture contents are 24.9, 28.6, 26.5, and 26.9 with an average of 26.7%. These moisture contents correspond to a moisture content of approximately 4.1% above the optimum moisture content.

Downloaded 01 May 2012 to 130.126.241.238. Redistribution subject to ASCE license or copyright. Visit http://www.ascelibrary.org

Table 1. Range of Compaction Parameters for Lifts 3–6 of the LPSL

Lift number	Range of dry unit weight (kN/m^3/pcf)	Standard proctor relative compaction	Range of compaction moisture content/average (%)	Moisture content above optimum (%)
3	15.0–15.9/95.3–101.0	95.0–100.0	22.8–26.5/25.0	1.2–4.9
4	15.1–15.3/95.8–97.4	95.5–97.1	23.2–25.5/24.2	1.6–3.9
5	15.0–15.3/95.5–97.5	95.3–97.2	22.3–26.7/25.4	0.7–5.1
6	15.0–15.7/95.4–100.1	95.1–99.8	21.6–26.7/26.0	0–5.1

Limit Equilibrium Analysis of Slide

Back-analysis of the observed sideslope instability was performed by using the computer program SLOPE/W and the following stability procedures: Janbu (1957), Spencer (1967), and Morgenstern and Price (1965) as coded in SLOPE/W. These stability procedures were used for the back-analyses because they satisfy all conditions of equilibrium and provide the best estimate of the factor of safety (Duncan and Wright 1980).

Analysis Cases

Back-Analysis of Slope Failure

A back-analysis was performed to estimate the shear resistance of the soil–soil interface in the compacted LPSL. In general, the slope geometry at the time of failure can be described as an average 3H:1V veneer fill slope over the natural weathered shale/sandstone subgrade. However, in the area of the slide, the slope inclination was 2.8H:1V or 19.6° slope (considering stockpiled protective cover materials) at the maximum elevation difference between the crest and toe of slope. The elevation difference between the crest and toe of the slope is approximately 31.5 m (103 ft), which is the vertical difference between the top of slope at or near elevation 229.4 m (752 ft) and the slope toe of elevation 197.9 m (649 ft). This geometry represents the conditions at the time of the slope failure and is illustrated in Fig. 7. For the back-analysis, the thickness of the protective sand was assumed to vary from 2.4 m (8 ft) at the crest to 0 m at two thirds of the slope as shown in Fig. 2.

Fig. 7 shows a LGP bulldozer operating on the slope that was modeled in SLOPE/W as a loaded area for the back-analysis. A seismic coefficient of 0.005 was used to model the vibration or acceleration effects of the dozer operating laterally on the slope as reported. In addition, a surcharge attributable to loaded trucks and stockpile material was included at the top of slope for this analysis.

Effective stress strength parameters for the compacted LPSL were measured by using consolidated undrained (CU) triaxial compression tests with pore pressure measurement on specimens obtained for prequalification sampling of the compacted LPSL. The CU triaxial tests yielded an effective stress friction angle (ϕ') of 19.5° for the LPSL. Given the slope angle in the slide area is 19.6°, it is not surprising that slope instability occurred, but it is surprising that the interface in the LPSL exhibited a lower shear resistance than the GM/LPSL interface because the factor of safety for an infinite slope can be simplified to the ratio of friction angle to slope angle as shown in the following:

$$\text{FS} = \frac{\tan\delta}{\tan\beta} = \frac{\tan(19.5°)}{\tan(19.6°)} = 0.99 \tag{1}$$

Strength parameters for the protective sand and the weathered bedrock were assumed because visual observations show that the failure plane was largely controlled by the compacted LPSL, and thus, the strength of the other materials did not play a significant role in the analysis. The material parameters used in the back-analysis are summarized in Table 2.

In the back-analysis, the reinforcement effect of the HDPE GM was considered by adopting the geofabric reinforcement option in the SLOPE/W. Koerner (1998) suggests an average peak tensile strength of a 60-mil textured HDPE GM in the machine direction of 23.1 kN/m. Therefore, the tensile resistance of the GM of 23.1 kN/m was used in the back-analysis because the GM was installed with the machine direction aligned down the slope. In addition, the interface friction angle for the GM/LPSL interface of 20.5° (Ling et al. 2001) was adopted assuming no adhesion occurs

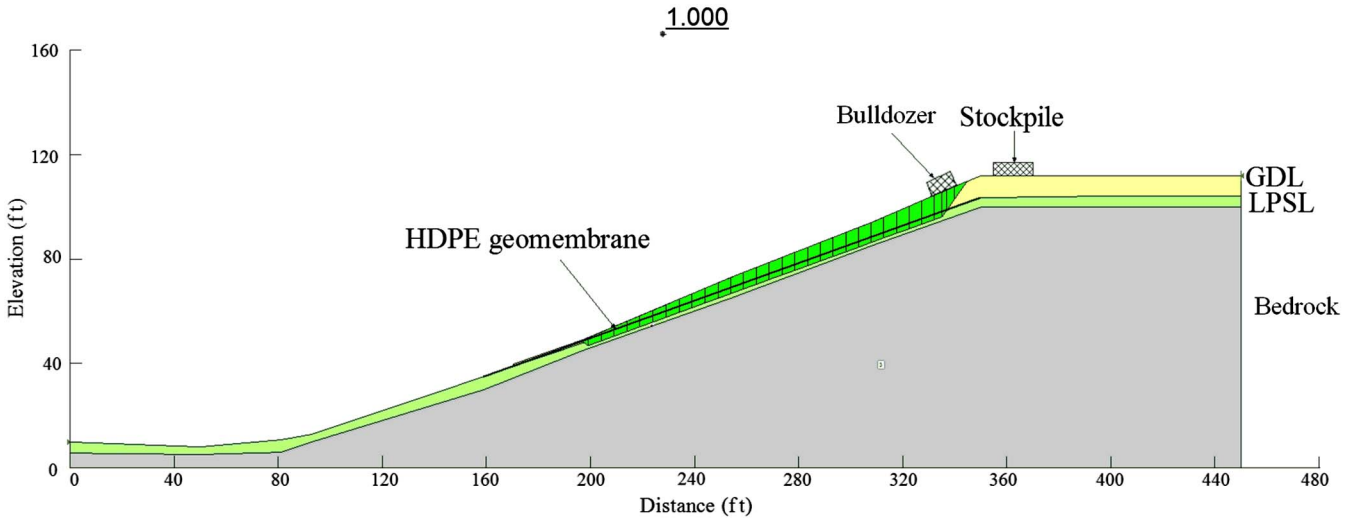

Fig. 7. Slope geometry before slide movement and back-analysis by using Morgenstern–Price's stability method

Downloaded 01 May 2012 to 130.126.241.238. Redistribution subject to ASCE license or copyright. Visit http://www.ascelibrary.org

Table 2. Material Properties for Back-Analysis

Material type	Total unit weight, γ_t (kN/m^3/pcf)	Cohesion, c' (kPa/psf)	Friction angle, ϕ' (°)
Lightly compacted protective sand	18.9/120	0	28
Compacted LPSL	19.5/124	13.4/280[a]	19.5
Underlying weathered soil/Bedrock	21.2/135	287.3/6,000	10

[a]Cohesion measured in CU triaxial compression test and reestimated in the back-analysis.

Table 3. Back-Calculated Cohesion Values for Compacted LPSL for Factor of Safety of Unity

Slope conditions	Dozer operation	Back-calculated cohesion value (kPa/psf) Janbu (1957)	Morgenstern and Price (1965)	Spencer (1967)
Surcharge and dump truck at crest	Side-to-side	1.25/26.0	1.14/23.8	0.70/14.6

on the GM/LPSL interface in the SLOPE/W back-analysis to consider all potential failure geometries.

It is assumed in the back-analysis that the critical parameter for the occurrence of the failure is the effective stress cohesion of the compacted LPSL. This assumption is on the basis of the low effective stress acting on the soil–soil interface in the LPSL, which results in a small contribution of shear resistance from the effective stress friction angle (ϕ') of 19.5°. Effective stress strength parameters were used in the analysis because the LPSL was not saturated because of the fact that the compaction moisture content ranged from 0.5 to 4.9% wet of optimum. The range of degree of saturation is from 80 to 92%.

In the back-analysis, effective stress cohesion of the compacted LPSL to achieve a factor of safety of unity (slope failure) was estimated. The slope geometry and failure surface used in the back-analysis with the Janbu (1957), Morgenstern and Price (1965), and Spencer (1967) stability procedures are also shown in Fig. 7, which shows the Morgenstern and Price back-analysis results. The back-calculated (or mobilized) effective stress cohesion values for the compacted LPSL are summarized in Table 3 for the Janbu, Morgenstern–Price, and Spencer stability procedures. Table 3 shows the back-calculated effective stress cohesion ranges from 0.70 to 1.25 kPa. The back-calculated values are significantly smaller than the effective stress cohesion obtained from the laboratory CU triaxial compression tests (13.4 kPa). The difference between the back-calculated and laboratory values of effective stress cohesion may be related to the difference in field (direct shear) and laboratory (triaxial) modes of shear, the triaxial specimen not having the weak soil–soil interface or the soil–soil interface not oriented properly in the triaxial device, and differences in moisture content and level of compaction between the field and laboratory.

In the additional slope stability analysis (the Morgenstern and Price method) with the same slope geometry and material properties including the back-calculated effective stress cohesion of 1.14 kPa, all potential failure geometries yielded a factor of safety greater than unity. Especially, the failure surface at the GM/LPSL interface provided a factor of safety of approximately 1.16 as shown in Fig. 8, which implies the slope failure would not occur at the GM/LPSL interface but would occur at the soil–soil interface within the LPSL.

In summary, this back-analysis provides a lower bound estimate of soil–soil interface effective stress cohesion (~1 kPa) that can develop in a LPSL for an effective stress friction angle of 19.5°.

Effect of Placing Cover Soil from Bottom to Top of Slope

For comparison purposes, another case was modeled that represents a better technique for placing the protective cover sand material over the GM. This technique involves starting soil placement at the slope toe and pushing the cover soil up the slope. This allows the cover soil at the slope toe to buttress the upslope material so that unsupported cover soil is not present on the slope. In this analysis, the protective cover thickness is assumed to be 0.6 m (2 ft) along the entire slope as shown in Fig. 9. Like the previous back-analysis, the tensile resistance of the GM ($T = 23.1$ kN/m) from Koerner (1998) and the interface friction angle for the GM/LPSL interface of 20.5° from Ling et al. (2001) were included in the analysis. Other differences in this model are as follows: (1) the protective cover material was not stockpiled at the slope crest, (2) the cover material was placed by using LGP equipment starting at the slope toe and moving straight up and down the slope instead of laterally across the slope, and (3) the equipment placing the cover material on the

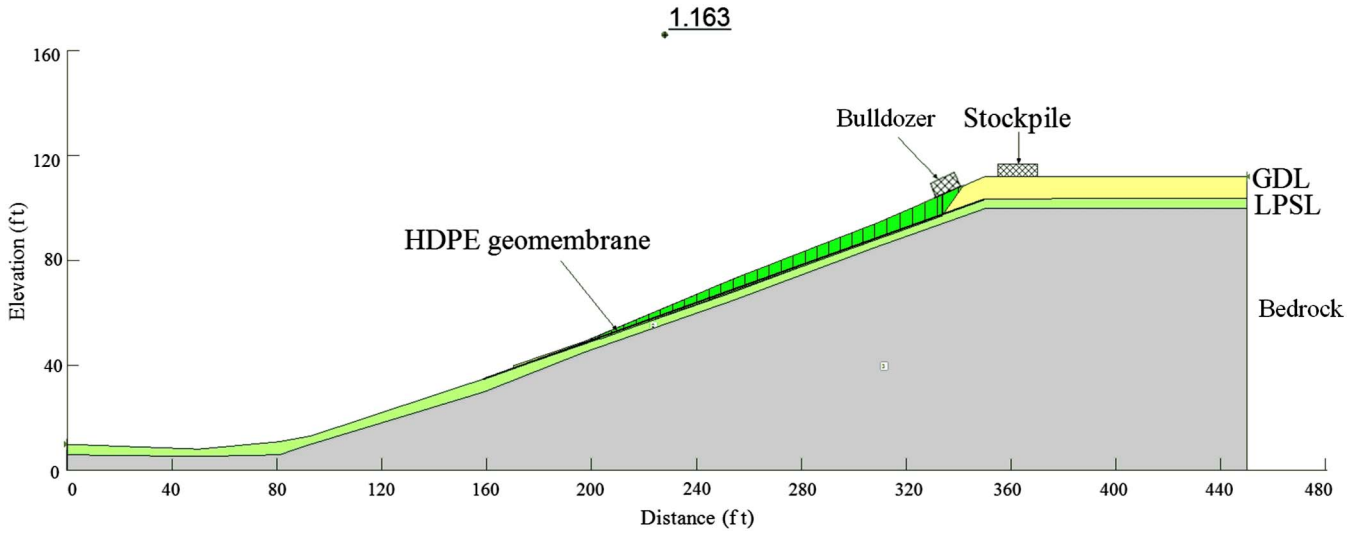

Fig. 8. Morgenstern–Price's stability analysis for failure surface at GM/LPSL interface

Downloaded 01 May 2012 to 130.126.241.238. Redistribution subject to ASCE license or copyright. Visit http://www.ascelibrary.org

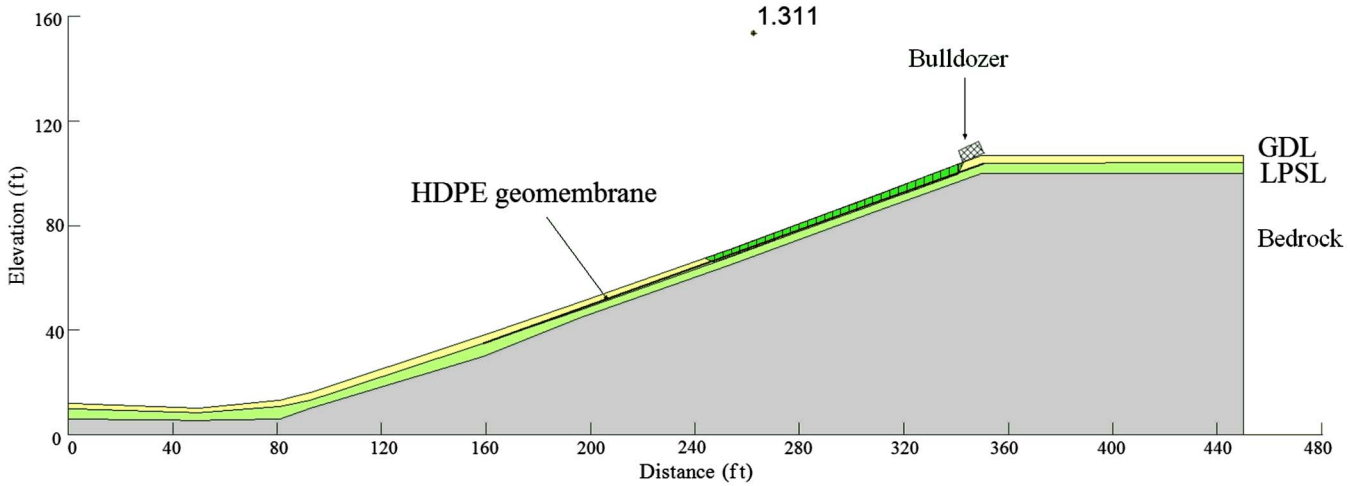

Fig. 9. Slope analysis by using the Morgenstern–Price method and soil placement from bottom to top of the slope

slope should keep material in front of the blade to a maximum height of 0.6 m (2 ft) above the surrounding material.

Strength parameters used in this analysis are the same as those in Table 1 except the back-calculated cohesion of 1.14 kPa (23.8 psf) for the compacted LPSL was adopted because Morgenstern and Price's procedure is more rigorous than the other two stability procedures. Fig. 9 shows the slope geometry and LGP equipment on the slope with cover soil placed from the bottom to the top of the slope and the slope geometry and critical failure surface for the Morgenstern and Price (1965) procedure, which yielded a factor of safety of approximately 1.31. The factors of safety for the Janbu (1957) and Spencer (1967) stability procedures are approximately 1.30 and 1.35, respectively, for soil placement from bottom to the top of the slope. Thus, placing the cover soil from the bottom to the top of the slope would have increased the factor of safety by approximately 40% so the slope probably would have been stable if the cover soil had been placed from the bottom to the top of the slope.

Geosynthetic Lined Slope Analyses

Giroud et al. (1995) present a limit equilibrium method to evaluate the stability of geosynthetic-soil layered systems of slopes. The main benefit of this method is the factor of safety is expressed by an equation that consists of the sum of the five terms as given in Eq. (2). This allows the contribution of various factors in the geosynthetic-soil layered system to be identified and quantified. For example, the first two terms of the equation represent the friction and adhesion strength parameters of the soil or geosynthetic interface. The next two terms of the equation represent the shear strength and geometry parameters for the soil buttress at the slope toe. The last term in Eq. (2) represents the geosynthetic tension of the geosynthetics in the slope. Therefore, the analysis using the method proposed by Giroud et al. (1995) directly includes the tensile resistance of the GM

$$\mathrm{FS} = \frac{\tan\delta}{\tan\beta} + \frac{a}{\gamma t \sin\beta} + \frac{t}{h} * \frac{\sin\phi}{\sin(2\beta)\cos(\beta+\theta)} + \frac{c}{\gamma h \sin\beta\cos(\beta+\theta)} + \frac{T}{\gamma h t} \quad (2)$$

where a = interface adhesion (kPa); δ = interface friction angle (°); c = soil cohesion (kPa); ϕ = soil friction angle (°); β = slope angle (°); t = thickness of soil cover (m); h = vertical height of slope (m); γ = unit weight of cover soil (kN/m^3); and T = geosynthetic tension (kN/m).

In the analysis of this slide, no soil buttress was included because the cover soil did not extend to the slope toe, that is, soil was pushed from the top to the bottom of the slope. As a result, the two soil buttress terms were removed from the factor of safety expression in Eq. (2) that suggests an average peak tensile strength of a 60-mil textured HDPE GM in the machine direction (the GM was installed with the machine direction aligned down the slope). Using Eq. (2), slope geometry parameters in Fig. 7, a tensile resistance of the GM of 23.1 kN/m from Koerner (1998), a GM/compacted LPSL interface friction angle of 20.5° from Ling et al. (2001), and assuming no adhesion occurs on the GM/LPSL interface, a factor of safety of 1.12 was calculated.

The analysis for stability of geosynthetic-soil layered systems of slopes by Giroud et al. (1995) yielded a factor of safety greater than unity in Eq. (2), which is consistent with field observations that the failure did not occur on the GM/compacted LPSL interface. Given the slope angle and LPSL interface friction angle are approximately 19.5° (2.8H:1V) in the slide area, the GM was probably placed in tension shortly after the cover soil was applied to the slope crest because the slope angle is at or exceeds the interface friction angle. Even though it appears the GM was placed in tension, sliding still occurred in the LPSL along a soil–soil interface. Accepted design practice is for geosynthetics to be designed without counting on any tensile resistance to prevent the development of progressive failure as probably occurred in this case.

Conclusion and Recommendations

The main conclusion and recommendations generated from this case history include the following:

- An interface in the compacted LPSL of a composite liner system can be weaker than the overlying GM/compacted LPSL interface, which is frequently the location of sliding.
- Designers and third-party CQA and CQC personnel should limit LPSL lift thickness so that the compaction equipment, for example, sheepsfeet, and compactive energy can penetrate the entire lift so a weak interface is not created in the LPSL that can lead to slope instability.
- New slope stability analyses should be performed whenever the field conditions differ from the design conditions, such as an increase in slope inclination and/or length. In this case, the

Downloaded 01 May 2012 to 130.126.241.238. Redistribution subject to ASCE license or copyright. Visit http://www.ascelibrary.org

design stability analyses represent a 3H:1V slope, but the overall slope in the slide was approximately 2.8H:1V, and the LPSL exhibited a lower strength than the GM interfaces, which were considered in the design.
- Cover soil placement should start at the slope toe and progress up the slope. This allows the cover soil at the slope toe to buttress the upslope material, so an infinite slope condition, that is, an unbuttressed slide block, does not develop and apply larger shear stresses to the interfaces and materials in the composite liner system.
- Low ground pressure equipment should be used to place the cover soil, and the equipment should move straight up and down the slope instead of laterally across the slope. This ensures that the equipment is supported by the previously placed soil instead of unsupported as the cover soil is pushed horizontally to an area that is not supported by prior placed cover soil.
- Slope angle on which cover soil is placed should not exceed the lowest geosynthetic or soil interface strength because progressive failure can occur along that interface and cause or lead to slope instability. At a minimum, this condition can lead to tension developing in the geosynthetics and damage to the geosynthetics and shear displacement occurring along the weak interface.

Acknowledgments

The authors acknowledge and appreciate the assistance of Luis Pazmino, a graduate research assistant at the University of Illinois at Urbana-Champaign, and Jeehee Lim, a graduate research assistant at Korea University, in finalizing this manuscript.

References

Amaya, P., Queen, B., Stark, T. D., and Choi, H. (2006). "Case history of liner veneer instability." *Geosynth. Int.*, 13(1), 36–46.

Bove, J. A. (1990). "Direct shear friction testing for geosynthetics in waste containment." *Proc., ASTM Symp. on Geosynthetic Testing for Waste Containment Applications*, Vol. 1081, ASTM, Philadelphia, 241–256.

Dixon, N., Jones, D. R. V., and Fowmes, G. J. (2006). "Interface shear strength variability and its use in reliability-based landfill stability analysis." *Geosynth. Int.*, 13(1), 1–14.

Dove, J. E., and Frost, J. D. (1999). "Peak friction behavior of smooth geomembrane–particle interfaces." *J. Geotech. Geoenviron. Eng.*, 125(7), 544–555.

Duncan, J. M., and Wright, S. G. (1980). "The accuracy of equilibrium methods of slope stability analysis." *Int. Symp. of Landslides*, New Delhi, India, 247–254 (also Engineering Geology, Vol. 16, Elsevier Scientific Publishing Amsterdam, The Netherlands, 5–17).

Giroud, J. P., Williams, N. D., Pelte, T., and Beech, J. F. (1995). "Stability of geosynthetic-soil layered systems on slopes." *Geosynth. Int.*, 2(6), 1115–1148.

Janbu, N. (1957). "Slope stability computations." *Embankment dam engineering, casagrande memorial volume*, E. Hirschfield and S. Poulos, eds., Wiley, New York, 47–86.

Koerner, R. M. (1998). *Designing with geosynthetics*, 4th Ed., Prentice Hall, Upper Saddle River, NJ.

Koerner, R. M., Martin, J. P., and Koerner, G. R. (1986). "Shear strength parameters between geomembranes and cohesive soils." *Geotext. Geomembr.*, 4(1), 21–31.

Koerner, R. M., and Soong, T.-Y. (1998). "Analysis and design of veneer cover soils." *Proc., 6th Int. Conf. on Geosynthetics—Giroud Lecture*, Vol. 1, IFAI, St. Paul, MN, 1–24.

Ling, H. I., Pamuk, A., Dechasakulsom, Mohri, Y., and Burke, C. (2001). "Interactions between PVC geomembranes and compacted clays." *J. Geotech. Eng.*, 127(11), 950–954.

Martin, J. P., Koerner, R. M., and Whitty, J. E. (1984). "Experimental friction evaluation of slippage between geomembrane, geotextiles, and soils." *Proc., Int. Conf. on Geomembranes*, Denver, IFAI, St. Paul, MN, 191–196.

Mitchell, J. K., Seed, R. B., and Seed, H. B. (1990). "Kettleman hills waste landfill slope failure I: Liner-system properties." *J. Geotech. Eng.*, 116(4), 647–668.

Morgenstern, N. R., and Price, V. E. (1965). "The analysis of the stability of general slip surfaces." *Geotechnique*, 15(1), 79–93.

Negussey, D., Wijewickreme, W. K. D., and Vaid, Y. P. (1989). "Geomembrane interface friction." *Can. Geotech. J.*, 26(1), 165–169.

O'Rourke, T. D., Druschel, S. J., and Netravali, A. N. (1990). "Shear strength characteristics of sand polymer interfaces." *J. Geotech. Eng.*, 116(3), 451–469.

Saxena, S. K., and Wong, Y. T. (1984). "Friction characteristics of a geomembrane." *Proc., Int. Conf. on Geomembranes*, IFAI, St. Paul, MN, 187–190.

Spencer, E. (1967). "A method of analysis of the stability of embankments assuming parallel inter-slice forces." *Geotechnique*, 17(1), 11–26.

Stark, T. D., Arellano, D., Evans, W. D., Wilson, V. L., and Gonda, J. M. (1998). "Unreinforced geosynthetic clay liner case history." *Geosynth. Int.*, 5(5), 521–544.

Stark, T. D., and Choi, H. (2004). "Peak versus residual interface strengths for landfill liner and cover design." *Geosynth. Int.*, 11(6), 491–498.

Stark, T. D., Choi, H., and McCone, S. D. (2005). "Drained strengths for analysis of landslides." *J. Geotech. Geoenviron. Eng.*, 131(5), 575–588.

Stark, T. D., and Poeppel, A. R. (1994). "Landfill liner interface strengths from torsional ring shear tests." *J. Geotech. Eng.*, 120(3), 597–615.

Stark, T. D., Williamson, T. A., and Eid, H. T. (1996). "HDPE geomembrane/geotextile interface shear strength." *J. Geotech. Eng.*, 122(3), 197–203.

Takasumi, D. L., Green, K. R., and Holtz, R. D. (1991). "Soil–geosynthetic interface strength characteristics: A review of state-of-the-art testing procedures." *Proc., of Geosynthetics '91 Conf.*, Vol. 1, IFAI, St. Paul, MN, 87–100.

Williams, N. D., and Houlihan, M. F. (1987). "Evaluation of interface friction properties between geosynthetics and soils." *Proc., Geosynthetics '87 Conf.*, Vol. 2, IFAI, St. Paul, MN, 616–627.

Yegian, M. K., and Lahlaf, A. M. (1992). "Discussion of Kettleman hills waste landfill slope failure I: Liner-system properties." *J. Geotech. Eng.*, 118(4), 643–645.

Downloaded 01 May 2012 to 130.126.241.238. Redistribution subject to ASCE license or copyright. Visit http://www.ascelibrary.org